Supporting Online Material

Abating HCl and HNO_3 is more effective than NH_3 for mitigating high aerosol loading over the Indo-Gangetic Plain

Prodip Acharja[1,2], Sachin D. Ghude[1*], Baerbel Sinha[3*], Mary Barth[4], Rachana Kulkarni[2], Vinayak Sinha[3], Rajesh Kumar[4], Kaushar Ali[1], Gaurav Govardhan[1], Ismail Gultepe[5,6,7], Madhavan Nair Rajeevan[8]

[1]Indian Institute of Tropical Meteorology, Ministry of Earth Sciences, India

[2]Savitribai Phule Pune University, Pune, India 411007

[3]Department of Earth and Environmental Sciences, Indian Institute of Science Education and Research Mohali, Punjab, India

[4]National Center for Atmospheric Research, Boulder, CO, 80307, USA

[5]ECCC, Meteorological Research Division, Toronto, Ontario, Canada

[6]Ontario Technical University, Engineering and Applied Science, Oshawa, Ontario, Canada

[7]Istinye University, Faculty of Engineering, Istanbul, Turkey

[8]Ministry of Earth Science, Lodhi Road, New Delhi, India

This file includes

Supplementary text

Table S1

Figure S1

Supporting Text

1. Data and measurements

1.1 Measurement site

The gas and particle-phase species measurements were conducted at the Indira Gandhi International Airport (IGIA), Delhi (28.56° N, 77.09°E, 237 m asl) under the Winter Fog Experiment (WiFEX) field campaign (Ghude et al., 2017). The measurement site fairly represents the general characteristics of highly polluted and densely populated urban locations in the IGP (Sinha et al., 2019; Ali et al., 2019). The measurements were conducted from 19 December 2017 to 10 February 2018 and a detailed description of the observation site and the prominent weather features associated with the winter period in Delhi has been well described in our earlier publications Ali et al., 2019; Acharja et al., 2021.

1.2 Instrumentation

1.2.1 Measurements of trace gases and inorganic constituents of PM_1, $PM_{2.5}$

In this study, the measurement of trace gases (HCl, HONO, HNO_3, SO_2, and NH_3) and the inorganic constituents (Cl^-, NO_3^-, SO_4^{2-}, Na^+, NH_4^+, K^+, Ca^{2+}, and Mg^{2+}) of fine particulates (PM_1 and $PM_{2.5}$) were simultaneously conducted at hourly resolution using Monitor for Aerosol and Gases in ambient Air (MARGA-2S, Make: Metrohm Applikon B.V, Netherlands) instrument (Rumsey et al., 2014).

The instrument is an assembly of equipment consisting of sampling unit, denuder for separating trace gases from the particles, aerosol collector, and analytical unit (Makkonen et al., 2012). MARGA-2S can provide a physicochemical characterization of particle matter along with trace gases on hourly time resolution (Schaap et al., 2011). In the measurement system, ambient air is first drawn through the PM_1, $PM_{2.5}$ inlets that pass through horizontal wet rotating denuder (WRD), and gases get diffused into an aqueous film. The aerosol gets collected in the steam jet aerosol collector (SJAC), where water-soluble aerosols grow in a supersaturated environment (Stieger et al., 2018). The water-soluble inorganic ions are quantified with two ion chromatography systems (anion + cation) using the principle presented by Oms et al., 1996. The MARGA-2S instrument was installed on the first floor of the building, whereas PM_1 and $PM_{2.5}$ impactors were installed on the terrace of the building nearly 8m above the ground and 2m above the roof surface. The instrument was continuously calibrated during its operation to ensure the quality of observation. A detailed description of

the MARGA-2S instrument, its operating principle, calibration method, and study location is discussed in our previous publication (Acharja et al., 2021). Meteorological parameters like temperature, relative humidity, wind speed, and wind direction were monitored with co-located automatic weather station (AWS).

2. Methodology

2.1 Thermodynamic equilibrium model ISORROPIA-II

The thermodynamic state of aerosols depends on ionic strength, dissociation of electrolyte, temperature of the solution, pH of aerosol, water activity, surface tension, density, and hygroscopicity (Kim et al., 1993; Tilgner et al., 2021). In the present study, ISORROPIA-II (Cl^- - NO_3^- - SO_4^{2-} - NH_4^+ - Na^+ - K^+ - Mg^{2+} - Ca^{2+} - H_2O system) model was used (Fountoukis and Nenes, 2007; Weber et al., 2016; Liu et al., 2017). In the model, the equilibrium is characterized by simultaneously considering a set of nonlinear algebraic equations coupled with appropriate electro-neutrality and mass conservation equations using the Newton-Raphson and bisectional methods (Ansari and Pandis., 1999). It is also assumed that the system is closed with respect to the total constituents, and the Gibbs free energy is at the global minimum. At this state, the variation in entropy concerning neighboring states is zero, and the system may remain at this energy level for arbitrarily long times.

The observational dataset of concentration of total ammonium (TNH_4=NH_3 + NH_4^+), total nitrate (TNO_3=HNO_3 + NO_3^-), and total chloride (TCl=HCl + Cl^-) along with Na^+, K^+, Ca^{2+}, and Mg^{2+} were used as inputs to run the model. The model can run in the "backward" mode based on the particle-phase data and in the "forward" mode based on the total (particle + gas) phase concentration data (Xu et al., 2015; Yao et al., 2007; Guo et al., 2017; Song et al., 2007). Studies have shown the "forward" mode to be more accurate and less sensitive to the measurement uncertainties compared to the "backward" mode (Hennigan et al., 2015; Bian et al., 2014). In the "forward" mode, the aerosols are assumed to exist in a metastable or aqueous state. These aqueous particles being larger than dry crystalline solids, generally scatter more light, degrade visibility, and influence mass transfer kinetics of trace gases (Rood et al., 1989).

The particle acidity (pH) is estimated using the following equation:

$$pH = -log_{10}\frac{1000 \times [H^+_{air}]}{ALWC} \quad (1)$$

where [H_{air}^+] concentration and aerosol liquid water content (ALWC) are the ISORROPIA-II model outputs (Liu et al., 2014; Xue et al., 2011). In the model, the ALWC was estimated by

considering the Raoult effect, curvature effect, and water uptake property (Bian et al., 2014; Hennigan et al., 2008). The water uptake of aerosols is calculated with the Zdanovskii–Stokes–Robinson (ZSR) hypothesis (Stokes and Robinson, 1966)

$$A = \sum_i \frac{M_i}{m_{oi}\,(a_w)} \qquad (2)$$

where M_i is the mole concentration of the electrolyte i (mol m^{-3}), $m_{oi}(a_w)$ is the corresponding molality of the binary solution of the electrolyte i under the same a_w (Seinfeld and Pandis, 2006). At the phase equilibrium a_w is equal to the ambient RH:

$$a_w = RH \qquad (3)$$

This approach ignores the contribution of organic species (e.g., oxalate, formate, acetate) to ALWC, but studies have shown that organics do not significantly affect the aerosol liquid water content (Ziemba et al., 2007; Malm and Day, 2001).

In this study, the data of RH in the 30–95% range were considered for the model simulation and data of RH > 95% were excluded since the exponential growth in ALWC with RH introduces large pH uncertainties (Guo et al., 2015). During the study period, the ambient humidity was high (≥50%), much higher than the efflorescence RH (10-30 %), so the "forward" mode consideration and the assumption that aerosols were in a completely deliquesced phase and remained at the "metastable" side of the hysteresis is reasonable. The model-derived pH of $PM_{2.5}$ was compared to make a comprehensive analysis of the model simulation.

2.2 Gas-particle partitioning ratio

The gas-to-particle partitioning and formation of secondary aerosols are significantly impacted by pH, ALWC, and T. High ALWC results in uptake of a gaseous species onto liquid and phase partitioning depending on the multiphase and heterogeneous reaction rates and the measurement or module of the model used (Nemitz et al., 2004; Hanson et al., 1994; Murphy et al., 2017). The partitioning ratio of ammonium [$\varepsilon(NH_4^+)$], nitrate [$\varepsilon(NO_3^-)$], and chloride [$\varepsilon(Cl^-)$] can be estimated using the following equations:

$$\varepsilon(NH_4^+) = \frac{[NH_4^+]}{[NH_3] + [NH_4^+]} \qquad (4)$$

$$\varepsilon(NO_3^-) = \frac{[NO_3^-]}{[HNO_3] + [NO_3^-]} \qquad (5)$$

$$\varepsilon(Cl^-) = \frac{[Cl^-]}{[HCl] + [Cl^-]} \quad (6)$$

where $[NH_4^+]$, $[NO_3^-]$, $[Cl^-]$, $[NH_3]$, $[HNO_3]$, [HCl] are the molar concentrations (μmol m^{-3}) of particulate and gaseous species respectively. The agreement between the predicted and measured partitioning ratios has been evaluated by estimating the mean bias (MB) and normalized mean bias (NMB) using the following equations:

$$MB = \frac{1}{N} \times \sum_{i=1}^{N} (M_i - O_i) \quad (7)$$

$$NMB = \frac{\sum_{i=1}^{N} (M_i - O_i)}{\sum_{i=1}^{N} O_i} \times 100\% \quad (8)$$

where, M_i and O_i are the model predicted and observed data, respectively, and N is the number of data points (Sudheer et al., 2015). These metrics are commonly used to evaluate the model predictions, and negative values for MB and NMB imply lower prediction, whereas positive values show the over-prediction.

2.3 Volume growth factor (VGF)

Factors like pH, ALWC, RH, aerosol composition, aerosol size, and aging of aerosol play an important role in visibility degradation by impacting the growth of hygroscopic aerosols (Stainer et al., 2003; Salcedo et al., 2006). The volume growth factor (VGF) is defined as the ratio of the volume of the wet particle to the corresponding volume of the dry particle (Zheng et al., 2015; Sun et al., 2013). Li et al., (2019) have discussed the size-independent VGF estimated using the following equation:

$$VGF = \frac{\frac{\sum m_{i.\ MARGA}}{\rho_i} + (\frac{ALWC_{inorg} + ALWC_{org})}{\rho_{water}}}{\frac{\sum m_{i.\ MARGA}}{\rho_i}} \quad (9)$$

where m_{iMARGA} is the mass concentration of species 'i' measured by MARGA-2S. In this calculation, we have also neglected the impact of organic fraction as studies have shown their growth is much less than water-soluble inorganic ions (Dusek et al., 2010; Petters and Kreidenweis, 2007; Guo et al., 2015). The major inorganic species are considered in the calculation, and the densities were assumed to be 1.52, 1.75, 1.75, 1.75, and 1.0 g cm^{-3} for chloride, nitrate, sulfate, ammonium, and water respectively (Salcedo et al., 2006).

3. Results and Discussions

3.1 Temporal evolution of pH and ALWC of PM_1 and $PM_{2.5}$

We explored the diurnal variation of pH and ALWC of PM_1 and $PM_{2.5}$ in Figure S1. ALWC increases from just after sunset to early morning, then decreases sharply due to daytime heating, increasing temperature, and decreasing RH. It reaches a maximum during morning traffic hours (08:00-10:00 hrs) due to high loadings of PM_1, $PM_{2.5}$ and high humidity in the shallow boundary layer. It was lowest in the afternoon, due to the combined effect of temperature and increased boundary layer height, which dilutes the particle concentration at the ground level, consistent with the variations in other polluted regions experiencing fog (Guo et al., 2018). The pH variation generally followed the variation of liquid water content and it showed a double peak, one in the morning (10:00 hrs), and another in the evening (20:00 hrs), as shown in Figure S1. It was minimum in the afternoon, similar to ALWC, and studies have shown the diurnal variation of ALWC to be the primary driving factor in the diurnal variation of pH.

3.2 Influence of RH and ALWC on volume growth factor (VGF)

In addition to controlling the pH of aerosols, ALWC also impacts the loading of aerosols where higher aerosol concentration increases ALWC content, further enhancing the multiphase formation of aerosol, especially when RH exceeded ≥ 80% resulting in the growth of aerosol during pollution events like fog (Su et al., 2020; Engelhart et al., 2011; Liu et al., 2011; Zhai et al., 2021). Limited research has been performed on this topic over IGP though the highest RH value was beyond 90% during the winter period.

Figures 3c, 3d give a clear view of VGF variability with RH. The figure shows that VGF of both PM_1 and $PM_{2.5}$ increased sharply when ambient RH was ≥ 70%, which is due to the water uptake by hygroscopic constituents. Below 70% RH, the mean PM_1 and $PM_{2.5}$ VGF is 2.02 ± 0.77, 2.08 ± 0.97, whereas at RH ≥ 70% the mean PM_1 and $PM_{2.5}$ VGF is 7.87 ± 4.58, 7.38 ± 4.46 respectively. This indicates the increment of VGF by 70% at higher RH, which can be attributed to the increased phase partitioning and formation of more SIA under fog (Sjogren et al., 2007; Wang et al., 2019).

During the whole measurement period, the average VGF of PM_1 and $PM_{2.5}$ was 4.83 ± 4.21, 5.05 ± 4.44 showing nearly 5 times increase in the volume of foggy particles compared to the particle volume at non-foggy conditions, which is consistent with previous studies (Bian et al., 2014). The increase in VGF of $PM_{2.5}$ aerosols was more compared to PM_1 as it has a larger volume fraction. This increased volume of particles at high RH would augment the particle mass loading, resulting in scattering more sunlight and lowering the surface temperature, and increasing fog sustenance. This results in a positive feedback

mechanism between RH and VGF that would reach equilibrium at some ALWC and pH (Wang et al., 2014; Guo et al. 2017).

Table S1. The measured total (gas + aerosol) concentration of chloride (TCl), nitrate (TNO_3), and ammonia (TNH_4) and estimated pH, ALWC, gas-to-particle partitioning ratio (ε) of ε (Cl^-), ε (NO_3^-), and ε (NH_4^+) of PM_1 and $PM_{2.5}$ during the WiFEX campaign period.

Variables	PM_1	$PM_{2.5}$
TNO_3 (μg m^{-3})	19.74 ± 9.81	31.67 ± 14.57
TCl (μg m^{-3})	22.28 ± 20.57	39.71 ± 35.41
TNH_4 (μg m^{-3})	43.41 ± 19.81	58.04 ± 24.06
Gas-to-particle partitioning ratio (ε)		
ε (Cl^-)	93 ± 09 %	96 ± 07 %
ε(NO_3-)	83 ± 11 %	89 ± 08 %
ε (NH_4^+)	42 ± 17 %	55 ± 15 %
Predicted from ISORROPIA-II		
pH	4.49 ± 0.53	4.58 ± 0.48
ALWC (μg m^{-3})	169 ± 205	324 ± 396

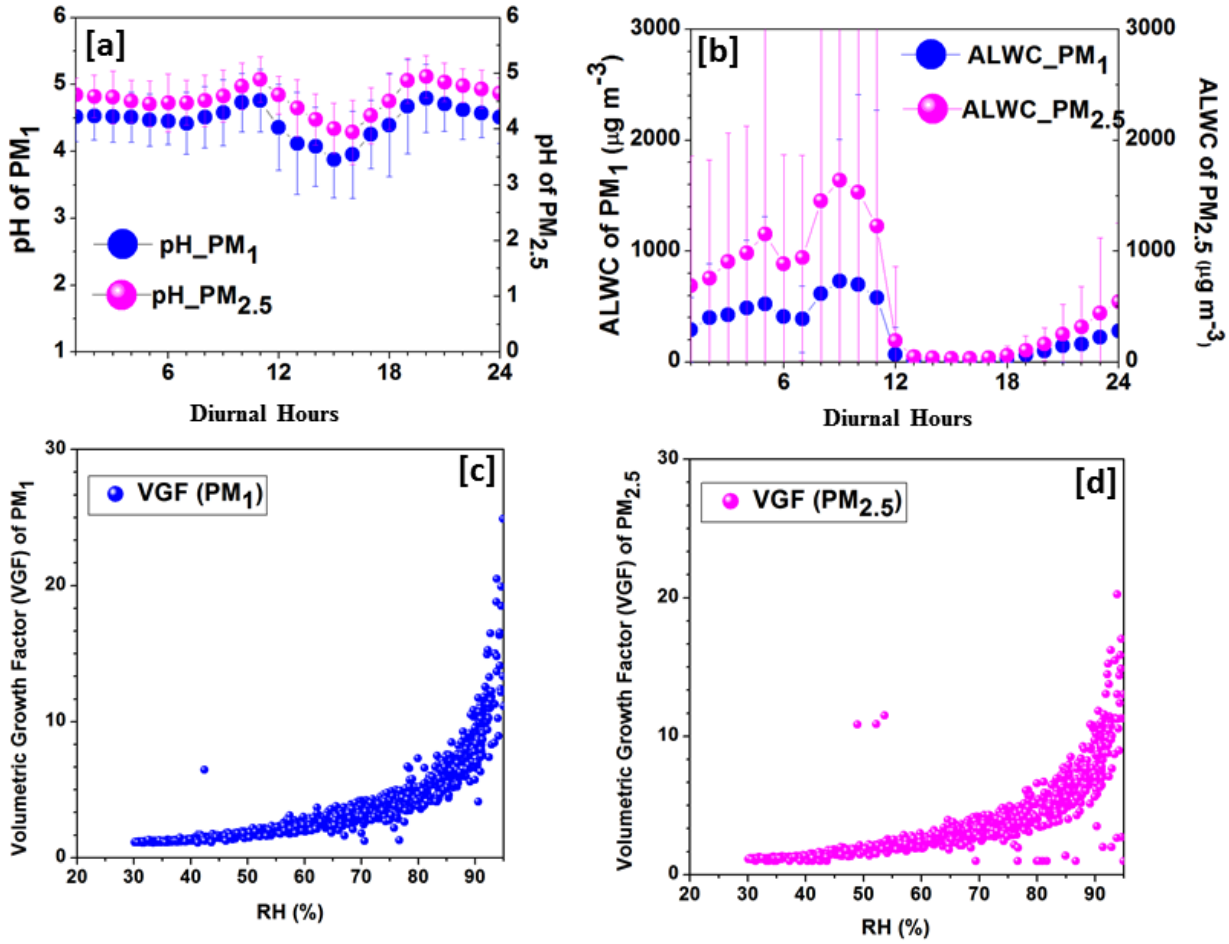

Figure S1: Diurnal variation of (a) pH and (b) ALWC of PM_1 and $PM_{2.5}$ predicted from the ISORROPIA-II model simulation. Variation of volume growth factor (VGF) of (c) PM_1 and (d) $PM_{2.5}$ as a function of RH during the WiFEX campaign period.

References

Acharja, P., Ali, K., Trivedi, D.K., Safai, P.D., Ghude, S., Prabhakaran, T. and Rajeevan, M., 2020. Characterization of atmospheric trace gases and water soluble inorganic chemical ions of PM1 and PM2. 5 at Indira Gandhi International Airport, New Delhi during 2017–18 winter. Science of the Total Environment, 729, p.138800.

Acharja, P., Ali, K., Ghude, S.D., Sinha, V., Sinha, B., Kulkarni, R., Gultepe, I. and Rajeevan, M.N., 2021. Enhanced secondary aerosol formation driven by excess ammonia during fog episodes in Delhi, India. Chemosphere, p.133155.

Ali, K., Acharja, P., Trivedi, D.K., Kulkarni, R., Pithani, P., Safai, P.D., Chate, D.M., Ghude, S., Jenamani, R.K. and Rajeevan, M., 2019. Characterization and source identification of PM2. 5 and its chemical and carbonaceous constituents during Winter Fog Experiment 2015–16 at Indira Gandhi International Airport, Delhi. Science of The Total Environment, 662, pp.687-696.

Ansari, A.S. and Pandis, S.N., 2000. The effect of metastable equilibrium states on the partitioning of nitrate between the gas and aerosol phases. Atmospheric Environment, 34(1), pp.157-168.

Bian, Y.X., Zhao, C.S., Ma, N., Chen, J. and Xu, W.Y., 2014. A study of aerosol liquid water content based on hygroscopicity measurements at high relative humidity in the North China Plain. Atmospheric Chemistry and Physics, 14(12), pp.6417-6426.

Dusek, U., Frank, G.P., Curtius, J., Drewnick, F., Schneider, J., Kürten, A., Rose, D., Andreae, M.O., Borrmann, S. and Pöschl, U., 2010. Enhanced organic mass fraction and decreased hygroscopicity of cloud condensation nuclei (CCN) during new particle formation events. *Geophysical Research Letters*, *37*(3).

Engelhart, G.J., Hildebrandt, L., Kostenidou, E., Mihalopoulos, N., Donahue, N.M. and Pandis, S.N., 2011. Water content of aged aerosol. Atmospheric Chemistry and Physics, 11(3), pp.911-920.

Guo, H., Otjes, R., Schlag, P., Kiendler-Scharr, A., Nenes, A. and Weber, R.J., 2018. Effectiveness of ammonia reduction on control of fine particle nitrate. Atmospheric Chemistry and Physics, 18(16), pp.12241-12256.

Hanson, D.R., Ravishankara, A.R. and Solomon, S., 1994. Heterogeneous reactions in sulfuric acid aerosols: A framework for model calculations. *Journal of Geophysical Research: Atmospheres*, *99*(D2), pp.3615-3629.

Hennigan, C.J., Izumi, J., Sullivan, A.P., Weber, R.J. and Nenes, A., 2015. A critical evaluation of proxy methods used to estimate the acidity of atmospheric particles. Atmospheric Chemistry and Physics, 15(5), pp.2775-2790.

Kim, Y.P., Seinfeld, J.H. and Saxena, P., 1993. Atmospheric gas-aerosol equilibrium I. Thermodynamic model. Aerosol Science and Technology, 19(2), pp.157-181.

Liu, M., Song, Y., Zhou, T., Xu, Z., Yan, C., Zheng, M., Wu, Z., Hu, M., Wu, Y. and Zhu, T., 2017. Fine particle pH during severe haze episodes in northern China. Geophysical Research Letters, 44(10), pp.5213-5221.

Makkonen, U., Virkkula, A., Mäntykenttä, J., Hakola, H., Keronen, P., Vakkari, V. and Aalto, P.P., 2012. Semi-continuous gas and inorganic aerosol measurements at a Finnish urban site: comparisons with filters, nitrogen in aerosol and gas phases, and aerosol acidity. *Atmospheric Chemistry and Physics*, *12*(12), pp.5617-5631.

Malm, W.C. and Day, D.E., 2001. Estimates of aerosol species scattering characteristics as a function of relative humidity. Atmospheric Environment, 35(16), pp.2845-2860.

Murphy, J.G., Gregoire, P.K., Tevlin, A.G., Wentworth, G.R., Ellis, R.A., Markovic, M.Z. and VandenBoer, T.C., 2017. Observational constraints on particle acidity using measurements and modelling of particles and gases. Faraday discussions, 200, pp.379-395.

Petters, M.D. and Kreidenweis, S.M., 2007. A single parameter representation of hygroscopic growth and cloud condensation nucleus activity. *Atmospheric Chemistry and Physics*, *7*(8), pp.1961-1971.

Rumsey, I.C., Cowen, K.A., Walker, J.T., Kelly, T.J., Hanft, E.A., Mishoe, K., Rogers, C., Proost, R., Beachley, G.M., Lear, G. and Frelink, T., 2014. An assessment of the performance of the Monitor for AeRosols and GAses in ambient air (MARGA): a semi-continuous method for soluble compounds. Atmospheric Chemistry and Physics, 14(11), pp.5639-5658..

Rood, M.J., Shaw, M.A., Larson, T.V. and Covert, D.S., 1989. Ubiquitous nature of ambient metastable aerosol. Nature, 337(6207), pp.537-539.

Salcedo, D., Onasch, T.B., Dzepina, K., Canagaratna, M.R., Zhang, Q., Huffman, J.A., DeCarlo, P.F., Jayne, J.T., Mortimer, P., Worsnop, D.R. and Kolb, C.E., 2006. Characterization of ambient aerosols in Mexico City during the MCMA-2003 campaign with Aerosol Mass Spectrometry: results from the CENICA Supersite. *Atmospheric Chemistry and Physics*, *6*(4), pp.925-946.

Sjogren, S., Gysel, M., Weingartner, E., Baltensperger, U., Cubison, M.J., Coe, H., Zardini, A.A., Marcolli, C., Krieger, U.K. and Peter, T., 2007. Hygroscopic growth and water uptake kinetics of two-phase aerosol particles consisting of ammonium sulfate, adipic and humic acid mixtures. Journal of Aerosol Science, 38(2), pp.157-171.

Sinha, B. and Sinha, V., 2019. Source apportionment of volatile organic compounds in the northwest Indo-Gangetic Plain using a positive matrix factorization model. Atmospheric Chemistry and Physics, 19(24), pp.15467-15482.

Schaap, M., Otjes, R.P. and Weijers, E.P., 2011. Illustrating the benefit of using hourly monitoring data on secondary inorganic aerosol and its precursors for model evaluation. Atmospheric Chemistry and Physics, 11(21), pp.11041-11053.

Song, S., Gao, M., Xu, W., Shao, J., Shi, G., Wang, S., Wang, Y., Sun, Y. and McElroy, M.B., 2018. Fine-particle pH for Beijing winter haze as inferred from different

thermodynamic equilibrium models. *Atmospheric Chemistry and Physics*, *18*(10), pp.7423-7438.

Stanier, C.O., Khlystov, A.Y., Chan, W.R., Mandiro, M. and Pandis, S.N., 2004. A Method for the In Situ Measurement of Fine Aerosol Water Content of Ambient Aerosols: The Dry-Ambient Aerosol Size Spectrometer (DAASS) Special Issue of Aerosol Science and Technology on Findings from the Fine Particulate Matter Supersites Program. *Aerosol science and technology*, *38*(S1), pp.215-228.

Stokes, R.H. and Robinson, R.A., 1966. Interactions in aqueous nonelectrolyte solutions. I. Solute-solvent equilibria. The Journal of Physical Chemistry, 70(7), pp.2126-2131.

Su, H., Cheng, Y. and Pöschl, U., 2020. New Multiphase Chemical Processes Influencing Atmospheric Aerosols, Air Quality, and Climate in the Anthropocene. *Accounts of Chemical Research*, *53*(10), pp.2034-2043.

Sudheer, A.K. and Rengarajan, R., 2015. Time-resolved inorganic chemical composition of fine aerosol and associated precursor gases over an urban environment in western India: gas-aerosol equilibrium characteristics. Atmospheric Environment, 109, pp.217-227.

Tilgner, A., Schaefer, T., Alexander, B., Barth, M., Collett Jr, J.L., Fahey, K.M., Nenes, A., Pye, H.O., Herrmann, H. and McNeill, V.F., 2021. Acidity and the multiphase chemistry of atmospheric aqueous particles and clouds. Atmospheric Chemistry and Physics Discussions, pp.1-82.

Wang, Y. and Chen, Y., 2019. Significant climate impact of highly hygroscopic atmospheric aerosols in Delhi, India. Geophysical Research Letters, 46(10), pp.5535-5545.

Weber, R.J., Guo, H., Russell, A.G. and Nenes, A., 2016. High aerosol acidity despite declining atmospheric sulfate concentrations over the past 15 years. *Nature Geoscience*, *9*(4), pp.282-285.

Xu, L., Guo, H., Boyd, C.M., Klein, M., Bougiatioti, A., Cerully, K.M., Hite, J.R., Isaacman-VanWertz, G., Kreisberg, N.M., Knote, C. and Olson, K., 2015. Effects of anthropogenic emissions on aerosol formation from isoprene and monoterpenes in the southeastern United States. *Proceedings of the National Academy of Sciences*, *112*(1), pp.37-42.

Yao, X., Ling, T.Y., Fang, M. and Chan, C.K., 2007. Size dependence of in situ pH in submicron atmospheric particles in Hong Kong. Atmospheric Environment, 41(2), pp.382-393.

Ziemba, L.D., Fischer, E., Griffin, R.J. and Talbot, R.W., 2007. Aerosol acidity in rural New England: Temporal trends and source region analysis. Journal of Geophysical Research: Atmospheres, 112(D10).